Integral equation based optimized Schwarz method for electromagnetics

Xavier Claeys[1], Bertrand Thierry[2], and Francis Collino[3]

1 Introduction

The optimized Schwarz method (OSM) is recognized as one of the most efficient domain decomposition strategies without overlap for the solution to wave propagation problems in harmonic regime. For the Helmholtz equation, this approach originated from the seminal work of Després [4, 5], and led to the development of an abundant literature offering more elaborated but more efficient transmission conditions, see [1, 6, 7, 8] and references therein. Most contributions focus on transmission conditions based on local operators.

In [2, 9, 10], the authors introduced non-local transmission conditions that can improve the convergence rate of OSM. In [9, Chap.8] the performance of this strategy was shown to remain robust up to GHz frequency range. Such an approach was proposed only for the Helmholtz equation, and has still not been adapted to electromagnetics.

In the present contribution we investigate such an approach for Maxwell's equations in a simple spherical geometry that allows explicit calculus by means of separation of variables. We study an Optimized Schwarz Method (OSM) where the transmission conditions are based on impedance type traces. The novelty lies in our impedance operator that we choose to be non-local. More precisely, it is chosen as a variant of the so-called Electric Field integral operator (see [11, §5.5]) where the wave number is purely imaginary. We show that the iterative solver associated to our strategy converges at an exponential rate.

1. Université Pierre et Marie Curie, and INRIA Paris, France. claeys@ann.jussieu.fr
2. CNRS and Université Pierre et Marie Curie, Paris, France. thierry@ljll.math.upmc.fr
3. POEMS (ENSTA ParisTech, CNRS, INRIA, Universit Paris-Saclay), Palaiseau, France. francis.collino@orange.fr

2 Maxwell's equations in harmonic regime

As a model problem we consider an electromagnetic transmission problem stemming from Maxwell's equations in harmonic regime where the whole space $\mathbb{R}^3$ is partitioned in two sub-domains $\mathbb{R}^3 = \overline{\Omega}_+ \cup \overline{\Omega}_-$ with Ω_- being the unit open ball centered at $\mathbf{0}$, and $\Omega_+ = \mathbb{R}^3 \setminus \overline{\Omega}_-$. Denote by $\boldsymbol{n}_\sigma$ the vector field normal to Γ directed toward the exterior of $\Omega_\sigma, \sigma = \pm$. With a constant wave number $\kappa > 0$, this is written

$$\begin{aligned}
&\boldsymbol{curl}(\boldsymbol{E}_\pm) - \imath\kappa \boldsymbol{H}_\pm = 0, \qquad \boldsymbol{curl}(\boldsymbol{H}_\pm) + \imath\kappa \boldsymbol{E}_\pm = 0 \quad \text{in } \Omega_\pm,\\
&\lim_{\rho\to\infty} \int_{\partial \mathrm{B}_\rho} |\boldsymbol{H}_+ \times \hat{\boldsymbol{x}} - \boldsymbol{E}_+|^2 \mathrm{d}\sigma_\rho = 0,\\
&\gamma_{\mathrm{T}}^+(\boldsymbol{E}) = +\gamma_{\mathrm{T}}^-(\boldsymbol{E}) + \boldsymbol{g}_{\mathrm{T}}\,, \qquad \text{with } \gamma_{\mathrm{T}}^\pm(\boldsymbol{E}) := \boldsymbol{n}_\pm \times (\boldsymbol{E}_\pm|_\Gamma \times \boldsymbol{n}_\pm),\\
&\gamma_{\mathrm{R}}^+(\boldsymbol{H}) = -\gamma_{\mathrm{R}}^-(\boldsymbol{H}) + \boldsymbol{g}_{\mathrm{R}}\,, \qquad \text{with } \gamma_{\mathrm{R}}^\pm(\boldsymbol{H}) := \boldsymbol{n}_\pm \times \boldsymbol{H}_\pm|_\Gamma,
\end{aligned} \tag{1}$$

with $\mathrm{B}_\rho := \{\boldsymbol{x} \in \mathbb{R}^3, |\boldsymbol{x}| < \rho\}$ and $\hat{\boldsymbol{x}} := \boldsymbol{x}/|\boldsymbol{x}|$. In this problem, $\boldsymbol{g}_{\mathrm{T}}, \boldsymbol{g}_{\mathrm{R}}$ are given source terms assumed to be supported on Γ only. Considering some invertible impedance operator $\mathcal{Z}$ that we shall define in Section 4, the transmission conditions in (1) can be reformulated as

$$\begin{aligned}
\gamma_{\mathrm{T}}^+(\boldsymbol{E}) + \mathcal{Z}\gamma_{\mathrm{R}}^+(\boldsymbol{H}) = \gamma_{\mathrm{T}}^-(\boldsymbol{E}) - \mathcal{Z}\gamma_{\mathrm{R}}^-(\boldsymbol{H}) + \boldsymbol{g}_{\mathrm{T}} + \mathcal{Z}\boldsymbol{g}_{\mathrm{R}},\\
\gamma_{\mathrm{T}}^-(\boldsymbol{E}) + \mathcal{Z}\gamma_{\mathrm{R}}^-(\boldsymbol{H}) = \gamma_{\mathrm{T}}^+(\boldsymbol{E}) - \mathcal{Z}\gamma_{\mathrm{R}}^+(\boldsymbol{H}) - \boldsymbol{g}_{\mathrm{T}} + \mathcal{Z}\boldsymbol{g}_{\mathrm{R}}.
\end{aligned} \tag{2}$$

For any tangential vector field $\boldsymbol{v}$ and $\sigma = \pm$ define the magnetic-to-electric operator $\mathcal{T}_\sigma(\boldsymbol{v}) := \gamma_{\mathrm{T}}^\sigma(\mathbf{U})$ where $(\mathbf{U}, \mathbf{V})$ is the unique solution to $\boldsymbol{curl}(\mathbf{U}) - \imath\kappa\mathbf{V} = 0$ in Ω_σ, $\boldsymbol{curl}(\mathbf{V}) + \imath\kappa\mathbf{U} = 0$ in Ω_σ and $\gamma_{\mathrm{R}}^\sigma(\mathbf{V}) = \boldsymbol{v}$ (and Silver-Müller's radiation condition if $\sigma = +$). Taking $\boldsymbol{u}_\sigma = \gamma_{\mathrm{T}}^\sigma(\boldsymbol{E}) + \mathcal{Z}\gamma_{\mathrm{R}}^\sigma(\boldsymbol{H}), \sigma = \pm$ as unknowns of our iterative procedure, Problem (1) is then equivalent to

$$\begin{aligned}
&\boldsymbol{u}_{-\sigma} = \mathcal{A}_\sigma(\boldsymbol{u}_\sigma) + \boldsymbol{f}_\sigma, \quad \sigma = \pm,\\
&\text{with } \mathcal{A}_\sigma := (\mathcal{T}_\sigma - \mathcal{Z})(\mathcal{T}_\sigma + \mathcal{Z})^{-1},
\end{aligned} \tag{3}$$

and $\boldsymbol{f}_\pm := (\mathcal{Z}(\boldsymbol{g}_{\mathrm{R}}) \pm \boldsymbol{g}_{\mathrm{T}})$. An optimized Schwarz strategy to solve Problem (1) now consists in a fixed point iterative method applied to (3), using the approximation $\boldsymbol{u}_\pm = \gamma_{\mathrm{T}}^\pm(\boldsymbol{E}) + \mathcal{Z}\gamma_{\mathrm{R}}^\pm(\boldsymbol{H}) = \lim_{n\to\infty} \boldsymbol{u}_\pm^{(n)}$ where $\boldsymbol{u}_\pm^{(n)}$ follows the recurrence

$$\begin{bmatrix} \boldsymbol{u}_+^{(n+1)} \\ \boldsymbol{u}_-^{(n+1)} \end{bmatrix} = \begin{bmatrix} 1-r & r\mathcal{A}_+ \\ r\mathcal{A}_- & 1-r \end{bmatrix} \cdot \begin{bmatrix} \boldsymbol{u}_+^{(n)} \\ \boldsymbol{u}_-^{(n)} \end{bmatrix} + \begin{bmatrix} r\boldsymbol{f}_+ \\ r\boldsymbol{f}_- \end{bmatrix}. \tag{4}$$

In this iterative method, $r > 0$ is a relaxation parameter whose effective value shall be discussed in the sequel.

3 Separation of variables on the sphere

To study the convergence of (4), we rely on the spherical symmetry of our model problem, and decompose the fields by means of vector spherical harmonics. According to e.g. [11, Thm.2.4.8], any tangential vector field $\boldsymbol{u} \in \mathrm{L}^2_{\mathrm{T}}(\Gamma) := \{\boldsymbol{v} : \Gamma \to \mathbb{C},\ \int_\Gamma |\boldsymbol{v}|^2 d\sigma < +\infty,\ \boldsymbol{x}\cdot\boldsymbol{v}(\boldsymbol{x}) = 0 \text{ on } \Gamma\}$ can be decomposed as

$$\boldsymbol{u}(\boldsymbol{x}) = \sum_{n=0}^{+\infty} \sum_{|m|\leq n} u^{\mathrm{D}}_{n,m}\, \mathbf{X}^{\mathrm{D}}_{n,m}(\boldsymbol{x}) + u^{\mathrm{C}}_{n,m}\, \mathbf{X}^{\mathrm{C}}_{n,m}(\boldsymbol{x}),$$
$$\text{with}\quad \mathbf{X}^{\mathrm{D}}_{n,m} := \tfrac{1}{\sqrt{n(n+1)}} \nabla_\Gamma \mathrm{Y}^m_n\ ,\quad \mathbf{X}^{\mathrm{C}}_{n,m} := \hat{\boldsymbol{x}} \times \mathbf{X}^{\mathrm{D}}_{n,m},$$

where $\hat{\boldsymbol{x}} := \boldsymbol{x}/|\boldsymbol{x}|$ and ∇_Γ is the surface gradient. Denoting $(\theta,\phi)\in[0,\pi]\times[0,2\pi]$ the spherical coordinates on Γ, spherical harmonics are defined by

$$\mathrm{Y}^m_n(\theta,\phi) := \sqrt{\frac{2n+1}{4\pi}}\sqrt{\frac{(n-|m|)!}{(n+|m|)!}}\ \mathrm{P}^{|m|}_n(\cos\theta)e^{\imath m\phi},$$

where $\mathrm{P}^{|m|}_n(t)$ are the associated Legendre functions, see e.g. [3, §2.3]. The tangent fields $\mathbf{X}^{\mathrm{D}}_{n,m}, \mathbf{X}^{\mathrm{C}}_{n,m}, 0 \leq |m| \leq n$ yield an orthonormal Hilbert basis of $\mathrm{L}^2_{\mathrm{T}}(\Gamma)$. The operators $\mathcal{T}_\pm$ are diagonalized by the functions $\mathbf{X}^{\mathrm{D}}_{n,m}, \mathbf{X}^{\mathrm{C}}_{n,m}$. Indeed we have $\mathcal{T}_\pm(\mathbf{X}^\star_{n,m}) = t^\star_{n,\pm}\mathbf{X}^\star_{n,m}$ for $\star = \mathrm{D},\mathrm{C}$ where, according to Formula (53) in [13],

$$\begin{aligned} t^{\mathrm{D}}_{n,-} &= 1/t^{\mathrm{C}}_{n,-} = +\imath\mathbb{J}'_n(\kappa)/\mathbb{J}_n(\kappa), \\ t^{\mathrm{D}}_{n,+} &= 1/t^{\mathrm{C}}_{n,+} = -\imath\mathbb{H}'_n(\kappa)/\mathbb{H}_n(\kappa). \end{aligned} \tag{5}$$

Here $\mathbb{J}_n(x) := \sqrt{\pi x/2}\ J_{n+1/2}(x)$ with $J_n(x)$ denoting the Bessel function of the first kind of order n, and $\mathbb{H}_n(x) := \sqrt{\pi x/2}\ H^{(1)}_{n+1/2}(x)$ with $H^{(1)}_n(x)$ denoting the Hankel function of the first kind of order n. The following result follows from [11, Thm.5.3.5].

Proposition 1.
We have $\Re e\{\int_\Gamma \overline{\boldsymbol{u}}\,\mathcal{T}_-(\boldsymbol{u})d\sigma\} = 0$ *and* $\Re e\{\int_\Gamma \overline{\boldsymbol{u}}\,\mathcal{T}_+(\boldsymbol{u})d\sigma\} > 0$ *for all* $\boldsymbol{u} \in \mathrm{L}^2_{\mathrm{T}}(\mathrm{div},\Gamma)\setminus\{0\}$ *where* $\mathrm{L}^2_{\mathrm{T}}(\mathrm{div},\Gamma) := \{\boldsymbol{v}\in\mathrm{L}^2_{\mathrm{T}}(\Gamma),\ \mathrm{div}_\Gamma(\boldsymbol{v})\in\mathrm{L}^2(\Gamma)\ \}$.

This result is related to energy balance in $\Omega_\pm$. With $\Re e\{\int_\Gamma \overline{\boldsymbol{u}}\,\mathcal{T}_-(\boldsymbol{u})d\sigma\} = 0$, the energy coming in Ω_- equals the outgoing energy. On the other hand, in Ω_+, there is energy radiated toward infinity as $\Re e\{\int_\Gamma \overline{\boldsymbol{u}}\,\mathcal{T}_+(\boldsymbol{u})d\sigma\} > 0$. A direct consequence in terms of separation of variables is

$$\Re e\{t^\star_{n,+}\} > \Re e\{t^\star_{n,-}\} = 0 \quad \text{for } \star = \mathrm{D},\mathrm{C},\ \forall n \geq 0. \tag{6}$$

That $\Re e\{t^{\star}_{n,-}\} = 0$ can also be seen directly from expression (5) since the $\mathbb{J}_n(z)$ are proportional to Bessel functions hence real valued. Assuming that the impedance is chosen so that $\mathcal{Z}(\mathbf{X}^{\star}_{n,m}) = z^{\star}_n\,\mathbf{X}^{\star}_{n,m}$ for $\star = \mathrm{D},\mathrm{C}$ and $n \geq 0$ where $z_{n,\star} \in \mathbb{C}$, we have

$$\mathcal{A}_{\pm}(\mathbf{X}^{\star}_{n,m}) = a^{\star}_{n,\pm}\,\mathbf{X}^{\star}_{n,m} \quad \text{with} \quad a^{\star}_{n,\sigma} = \frac{t^{\star}_{n,\sigma} - z^{\star}_n}{t^{\star}_{n,\sigma} + z^{\star}_n}. \tag{7}$$

The exponential convergence of the optimized Schwarz method is guaranteed provided that the spectral radius ϱ_{OSM} of the iteration operator in (4) is strictly smaller than 1,

$$\varrho_{\mathrm{OSM}} = \sup_{n\geq 0} \varrho_n < 1, \quad \text{with } \varrho_n := \max_{\sigma=\pm,\star=\mathrm{D},\mathrm{C}} |1 - r \pm r\sqrt{a^{\star}_{n,+}a^{\star}_{n,-}}|. \tag{8}$$

First observe that, for any $r \in (0,1)$, we have $|1 - r + r\lambda| < 1$ as soon as $\lambda \neq 1$ and $|\lambda| \leq 1$. Since $|(z-1)/(z+1)| \leq 1$ if and only if $\Re e\{z\} \geq 0$, a necessary condition of convergence is that $\varrho_n < 1$ for each n which boils down to $\Re e\{t^{\star}_{n,\sigma}/z^{\star}_n\} \geq 0$ for each $n, \sigma, \star$. According to (6), the later condition holds provided that $z^{\star}_n \in (0,+\infty)$.

4 Non-local impedance operator

Now let us discuss our construction of the impedance operator $\mathcal{Z}$. Compared to existing literature on optimized Schwarz strategies in the context of electromagnetics, the peculiarity of the present contribution lies in our choice of $\mathcal{Z}$ that is non-local. We choose

$$\mathcal{Z}(\boldsymbol{u}) := \alpha \int_{\Gamma} \mathcal{G}_{\alpha}(\boldsymbol{x}-\boldsymbol{y})\boldsymbol{u}(\boldsymbol{y})d\sigma(\boldsymbol{y}) - \frac{1}{\alpha}\nabla_{\Gamma}\int_{\Gamma} \mathcal{G}_{\alpha}(\boldsymbol{x}-\boldsymbol{y})\mathrm{div}_{\Gamma}\boldsymbol{u}(\boldsymbol{y})d\sigma(\boldsymbol{y}) \tag{9}$$

where the kernel $\mathcal{G}_{\alpha}(\boldsymbol{x}) := \exp(-\alpha|\boldsymbol{x}|)/(2\pi|\boldsymbol{x}|)$ satisfies $-\Delta\mathcal{G}_{\alpha} + \alpha^2\mathcal{G}_{\alpha} = 2\delta_0$ in $\mathbb{R}^3$, and $\alpha > 0$ is a parameter whose value shall be discussed later. The operator given by (9) is a classical object of potential theory that can be understood as a dissipative version of the so-called Electric Field Integral operator (EFIE). Defined in this manner, the operator $\mathcal{Z}$ is diagonalized by the $\mathbf{X}^{\star}_n$. According to Formula (54) in [13] we have

$$z^{\mathrm{D}}_n = 2\mathbb{J}'_n(\imath\alpha)\mathbb{H}'_n(\imath\alpha) \quad \text{and} \quad z^{\mathrm{C}}_n = 2\mathbb{J}_n(\imath\alpha)\mathbb{H}_n(\imath\alpha). \tag{10}$$

According to Rayleigh's formulas, see [12, Chap.10], we have $\mathbb{J}_n(\imath x) = (\imath x)^{n+1}$ $(x^{-1}\partial_x)^n(\sinh(x)/x)$ and $\mathbb{H}_n(\imath x) = -(\imath x)^{n+1}(x^{-1}\partial_x)^n(\exp(-x)/x)$. It is clear from (10) that $z^{\mathrm{D}}_n, z^{\mathrm{C}}_n > 0$ for all $n \geq 0$.

Satisfying $\varrho_n < 1$ for each n is necessary but not sufficient for (8) to be fulfilled. We must also verify that $\limsup_{n\to\infty} \varrho_n < 1$. Let us study the asymptotic behaviour of ϱ_n for $n \to \infty$. First, observe that (5) and (10) provide explicit expressions for $z_n^\star$ and $t_{n,\sigma}^\star$ where $\star = \mathrm{D}, \mathrm{C}$ and $\sigma = \pm$. According to [3, §2.4], we have $\mathbb{J}_n(x) \sim x^{n+1} n! 2^n/(2n+1)!$ and $\mathbb{H}_n(x) \sim -\imath x^{-n}(2n)!/(n! 2^n)$ for $n \to +\infty$, and these asymptotics hold for both $x \in \mathbb{R}$ and $x \in \imath\mathbb{R}$. Plugging this inside (5) and (10) yields, for $n \to +\infty$,

$$z_n^{\mathrm{D}} \underset{n\to\infty}{\sim} \frac{n}{\alpha}, \quad z_n^{\mathrm{C}} \underset{n\to\infty}{\sim} \frac{\alpha}{n} \quad \text{and} \quad t_{n,\pm}^{\mathrm{D}} \underset{n\to\infty}{\sim} \frac{\imath n}{\kappa}.$$

We also deduce the asymptotics of $t_{n,\pm}^{\mathrm{C}} = 1/t_{n,\pm}^{\mathrm{D}}$. From this we obtain $t_{n,\pm}^{\mathrm{D}}/z_n^{\mathrm{D}} \sim \imath\alpha/\kappa$ and $t_{n,\pm}^{\mathrm{C}}/z_n^{\mathrm{C}} \sim -\imath\kappa/\alpha$. With (7) we conclude that

$$\lim_{n\to\infty} a_{n,\pm}^{\mathrm{D}} = +\phi(\alpha/\kappa) \quad \text{and} \quad \lim_{n\to\infty} a_{n,\pm}^{\mathrm{C}} = -\phi(\alpha/\kappa) \;\; \text{where } \phi(\gamma) := \frac{\imath\gamma - 1}{\imath\gamma + 1}.$$

Now we have $\lim_{n\to\infty} \varrho_n = \max |\, 1 - r \pm r\phi(\alpha/\kappa)\,|$. A natural idea for choosing the parameters r and α consists in minimizing this quantity. The minimum is obtained for $\alpha = \kappa$ and $r = 1/2$ and we have in this case (note that this limit does not depend on κ)

$$\lim_{n\to\infty} \varrho_n = 1/\sqrt{2} \qquad \text{for } \alpha = \kappa,\ r = 1/2. \tag{11}$$

The control of ϱ_n when n goes to infinity is crucial to obtain geometrical convergence. It cannot be obtained when the impedance operator is a combination of local operators (with Padé approximants of the true impedance for instance). The use of non-local and positive impedance operator is the price to pay to achieve geometrical convergence.

5 Numerical illustration

Below we illustrate our analysis with effective numerical calculation[1] of the eigenvalues of the iteration operator of (4), taking systematically $\alpha = \kappa$. In Fig.1 below, we plot these eigenvalues for $\kappa = 10$. We see that the whole spectrum is contained in the unit disc. The values $\pm\imath$ clearly appear as the accumulation points of the spectrum with no relaxation ($r = 1$).

For eigenvalues associated to the relaxation parameter $r = 1/2$, we see that the accumulation points are located at $(1/2, \pm 1/2)$ whose modulus is $1/\sqrt{2}$, which agrees with (11). Next, in Fig.2 we show the same plots at higher frequency $\kappa = 100$. Once again, the whole spectrum is contained in the unit disc.

[1] Matlab scripts are available at: `http://gitlab.lpma.math.upmc.fr/IEOSM/Matlab`

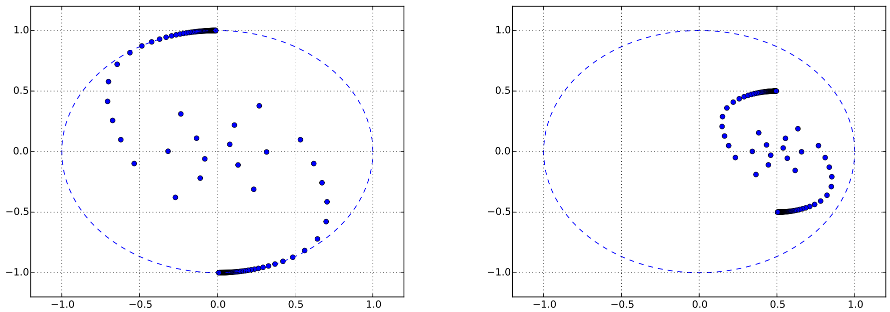

Fig. 1: Iteration eigenvalues with $\kappa = 10$ for $r = 1$ (left) and $r = 1/2$ (right)

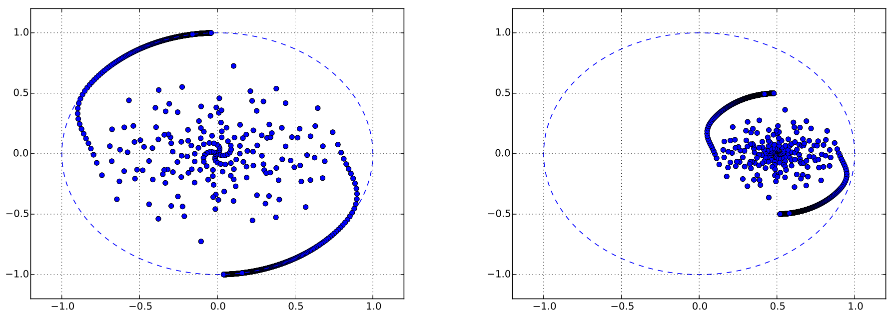

Fig. 2: Iteration eigenvalues with $\kappa = 100$ for $r = 1$ (left) and $r = 1/2$ (right)

Finally in Fig.3 we plot the values ϱ_n versus the modal index n for $\kappa = 10, 30, 100$. For low modal indices, it oscillates with growing amplitude until it reaches a pick located around $n \sim \kappa$. Then ϱ_n smoothly decays to $1/\sqrt{2}$. This scenario does not change as κ grows.

Although $\lim_{n\to\infty} \varrho_n$ remains independent of κ, the spectral radius $\sup_{n\geq 0} \varrho_n$ (reached around $n = \kappa$) does depend on κ, and we see in Fig.3 that this maximum grows closer to 1 as $\kappa \to \infty$. This suggests us that the values $\alpha = \kappa$ and $r = \frac{1}{2}$ may not be the optimal choice.

6 Conclusion

We have shown the convergence of the domain decomposition algorithm based on a dissipative EFIE transmission condition. How to choose the parameter α in a more optimal way should be further investigated. Moreover, it would be worth examining variants of the transmission operator (9). Augmenting it with additional local terms based on Padé approximants, in the manner of [6], seems promising.

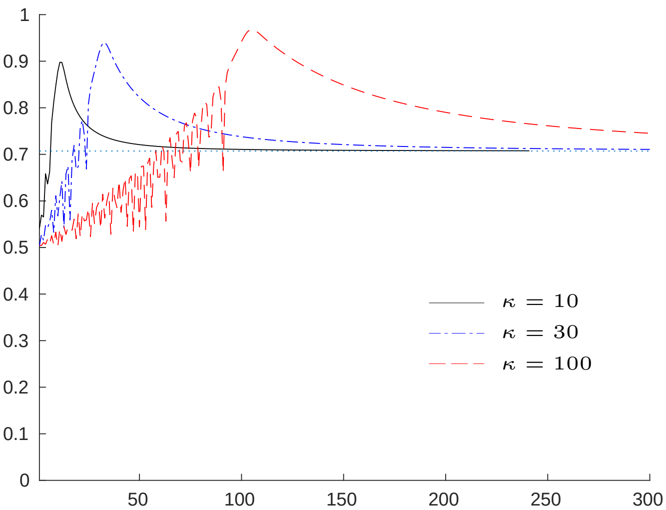

Fig. 3: Values of ϱ_n versus n with $r = 0.5$ for $\kappa = 10, 30, 100$.

Besides, in a finite element context, the use of a non-local operator is expensive in terms of both CPU time and memory storage. Various approaches could be considered for overcoming this problem. A possible solution may consist in truncating the Green kernel so as to (quasi)-localize the operator. The choice of the truncation and how it impacts the iteration operator should then be further investigated.

Other extensions of the present work are possible. For non-spherical interfaces, using the approach developed in [2], a convergent strategy would be obtained by choosing the impedance operator according to (9). This remark also holds in the case of multiple sub-domains, as long as there is no junction point at interfaces. Our strategy can also be adapted to the case of piecewise constant material characteristics. For this case also, the theory in [2] suggests that our method is convergent although, this time, a choice of impedance operator that varies according to the sub-domains may be more optimal. Finally the case of fully heterogeneous media seems to be still a widely open question.

Acknowledgment This work received support from the ANR research Grant ANR-15-CE23-0017-01.

References

[1] Y. Boubendir, X. Antoine, and C. Geuzaine. A quasi-optimal non-overlapping domain decomposition algorithm for the Helmholtz equation. *J. Comput. Phys.*, 231(2):262–280, 2012.

[2] F. Collino, S. Ghanemi, and P. Joly. Domain decomposition method for harmonic wave propagation: a general presentation. *Comput. Methods Appl. Mech. Engrg.*, 184(2-4):171–211, 2000.

[3] D. Colton and R. Kress. *Inverse acoustic and electromagnetic scattering theory*, volume 93 of *Applied Mathematical Sciences*. Springer, New York, third edition, 2013.

[4] B. Després. Décomposition de domaine et problème de Helmholtz. *C. R. Acad. Sci. Paris Sér. I Math.*, 311(6):313–316, 1990.

[5] B. Després. *Méthodes de décomposition de domaine pour les problèmes de propagation d'ondes en régime harmonique. Le théorème de Borg pour l'équation de Hill vectorielle*. 1991. PhD thesis, Univ. de Paris IX (Dauphine), 1991.

[6] M. El Bouajaji, B. Thierry, X. Antoine, and C. Geuzaine. A quasi-optimal domain decomposition algorithm for the time-harmonic Maxwell's equations. *J. Comput. Phys.*, 294:38–57, 2015.

[7] M. J. Gander. Optimized Schwarz methods for Helmholtz problems. In *Domain decomposition methods in science and engineering (Lyon, 2000)*, Theory Eng. Appl. Comput. Methods, pages 247–254. Internat. Center Numer. Methods Eng. (CIMNE), Barcelona, 2002.

[8] M.J. Gander, F. Magoulès, and F. Nataf. Optimized Schwarz methods without overlap for the Helmholtz equation. *SIAM J. Sci. Comput.*, 24(1):38–60, 2002.

[9] M. Lecouvez. *Iterative domain decomposition method without overlap with geometric convergence for Helmholtz equation*. Phd thesis, École Polytechnique, 2015.

[10] M. Lecouvez, B. Stupfel, P. Joly, and F. Collino. Quasi-local transmission conditions for non-overlapping domain decomposition methods for the helmholtz equation. *Comptes Rendus Physique*, 15(5):403 – 414, 2014.

[11] J.-C. Nédélec. *Acoustic and electromagnetic equations*, volume 144 of *Applied Mathematical Sciences*. Springer-Verlag, New York, 2001.

[12] F. W. J. Olver, D. W. Lozier, R. F. Boisvert, and C. W. Clark, editors. *NIST handbook of mathematical functions*. Cambridge University Press, Cambridge, 2010.

[13] F. Vico, L. Greengard, and Z. Gimbutas. Boundary integral equation analysis on the sphere. *Numer. Math.*, 128(3):463–487, 2014.